On the Impact of Measurement Errors on Power System Automatic Generation Control

Jiangmeng Zhang, *Student Member, IEEE,* and Alejandro. D. Domínguez-García, *Member, IEEE*

***Abstract*—In this paper, we propose a framework to evaluate the impact on power system dynamic performance of different types of errors in the measurements utilized by the automatic generation control (AGC) system. To address the random nature of these errors, stochastic system analysis methods are utilized to evaluate the statistics of system state variables. By examining the convergence properties of these statistics, errors that cause instability are identified. A reduced-order model, obtained by using singular perturbation arguments, is also formulated that enables us to provide analytical expressions capturing the impact of the errors. The proposed method is illustrated and verified through several case studies with different types of errors on a simplified New England/New York system model.**

***Index Terms*—Power system automatic generation control, measurement errors, power system stability**

I. Introduction

Measurement integrity is paramount in power system operations and control. However, measurement errors are inevitable due to miscellaneous phenomena, e.g., measuring device malfunction and noise in communication channels. Furthermore, measurement data are also vulnerable to intentional cyber attacks, which can introduce engineered errors and, in turn, may significantly degrade system dynamic performance. In this regard, vulnerabilities due to cyber attacks in power system control and data acquisition systems have been extensively documented (see e.g., [1]). Therefore, it is critical to comprehensively evaluate the impact of different types of measurement errors so as to identify critical ones.

In this work, we consider the impact of errors, some of which can be caused by cyber attacks, in the measurements utilized by the automatic generation control (AGC) system, which is currently the only system-level closed-loop control system across both the cyber and physical layers of a power system [2]. As part of the supervisory control and data acquisition (SCADA) system, the AGC algorithms are implemented in a centralized location (typically a control center). AGC is critical for power systems to (i) regulate frequency, and (ii) keep the power interchange between balancing authority (BA) areas at the scheduled values. To achieve these goals, the AGC system takes measurements of: (i) the area frequency, (ii) the generation output of committed units, and (iii) the tie-line power flow between BA areas; calculates the so-called area control error (ACE); and determines the generator set point values so as to drive the ACE to zero. These measurements acquired at various points of the physical power system network are transmitted to the control center over a cyber network. It is obvious then that measurement data quality is critical to system performance in the sense that measurement errors (e.g., false data injection over the communication channels) may mislead the calculation involved in the AGC algorithms, and severely affect the overall system performance.

From the perspective of erroneous measurement types, measurement data can be delayed (e.g., due to excessive communication traffic or denial of service attacks, see [3], [4]); manipulated (e.g., due to man-in-the-middle attacks, see [5]); or even lost (e.g., through a lossy network, see [6], [7]). From the perspective of assessing the impact of erroneous measurements, [8] presents a class of false data injection attacks that can modify the estimated system state in arbitrary ways. The authors of [9] evaluate the effects of erroneous measurements on the power market. The authors of [10] investigate an integrity attack on the measurements used in the AGC system performance to mislead the operator to perform inappropriate control actions, which may subsequently trigger improper actions (e.g., load shedding, or generator isolation), and even cause cascading failures. Finally, [4] investigates whether the system will preserve stability at all with introduced measurement errors.

In this paper, we classify measurement errors as *deterministic* and *random*. While most previous works focus on deterministic errors, in this work, we develop an analytical evaluation framework that can capture random measurement errors as well. Building on our previous results reported in [11], we propose a stochastic differential equation (SDE) framework to capture the system dynamics under random phenomena (due to measurement errors). Then, we apply analysis techniques proposed in [12] to evaluate the statistics of the system state variables (such as frequency). This allows us to investigate system stability when measurements are corrupted with both deterministic and random errors, and identify a class of errors with critical parameter values that cause unsatisfactory system performance and even loss of stability.

As an extension of [11], we propose an analytically tractable method to examine the impact of different erroneous measurements (e.g., errors in frequency measurements, and errors in generation output measurements), and to explicitly identify critical parameter values. To this end, we utilize singular perturbation arguments to derive a reduced-order model of the system dynamics. To this end, we assume that the AGC

The authors are with the Department of Electrical and Computer Engineering, University of Illinois at Urbana-Champaign, Urbana, IL 61801 USA (e-mail: jzhang67@illinois.edu; aledan@illinois.edu).

This work was supported in part by the Trustworthy Cyber Infrastructure for the Power Grid (TCIPG) under U.S. Department of Energy award DE-OE0000097, the National Science Foundation (NSF) under grant ECCS-CPS-1135598, and by the Consortium for Electric Reliability Technology Solutions (CERTS).

dynamics dominate the system dynamic behavior in the time scale of interest. With this model, we can analytically examine the impact of different erroneous measurement variables. Frequency measurement errors are shown to be critical to system stability. We show that although errors in generation output measurements will not affect the system stability characteristics, they can significantly degrade system performance. The accuracy of the reduced-order model is verified through a case study, involving a 68-bus model of the New England/New York power system. Specifically, we consider (i) a comprehensive model capturing the power system electromechanical dynamics and AGC dynamics (i.e., a full-order model), and (ii) a reduced-order model obtained under the aforementioned assumption. For each of these models, we identify the range of error parameter values that destabilize the system. As expected, the parameter value range identified using the reduced-order model is a close approximation of that identified using the full-order model.

The remainder of this paper is organized as follows. Section II presents the modeling framework, including the power system electromechanical dynamics model, the AGC sytem model, and the measurement model. Section III describes the proposed assessment method. Section IV showcases the analysis framework using the reduced-order model obtained from singular perturbation arguments. Section V discusses some issues with practical AGC systems, as well as some ideas for detection and mitigation. Section VI illustrates the analysis framework on a 68-bus power system. Concluding remarks are presented in Section VII.

II. Modeling Framework

In this section, we present the modeling framework adopted in this work, which includes the standard power-system electromechanical dynamics differential algebraic equation (DAE) model, the AGC system model, and the measurement model.

A. Power System Electromechanical Dynamics Model

We describe the electromechanical behavior of a power system by a set of DAEs of the form (see, e.g., [13], [14]):

$$\dot{x} = f(x, y, u), \tag{1a}$$

$$0 = g(x, y), \tag{1b}$$

where $x(t) \in \mathbb{R}^n$ contains the dynamic states of synchronous generators; $y(t) \in \mathbb{R}^m$ denotes the system algebraic states, including bus voltage magnitudes and angles; $u(t) \in \mathbb{R}^l$ includes generator set points; $f : \mathbb{R}^{n+m+l} \mapsto \mathbb{R}^n$ describes the evolution of the dynamics states; and $g : \mathbb{R}^{n+m} \mapsto \mathbb{R}^m$ describes the power flow equations.

B. Automatic Generation Control Model

The governor set points u, in (1a), are determined by a secondary frequency control system referred to as automatic generation control (AGC). The function of the AGC system is to reduce the generation and demand mismatch so as to maintain the system frequency at its nominal value, e.g., 60 Hz in North America, and to maintain the net power flow in tie lines across different balancing authority (BA) areas at its scheduled value. To achieve these objectives, the AGC system takes measurements of (i) the frequency in each BA area, (ii) the tie-line power flow between BA areas, and (iii) the generator output, and calculates the ACE to determine the generator set points.

Let $P_{aa'}^{meas}$ denote the measured power interchange from area a to a neighboring area a', $P_{aa'}^{sch}$ denote the scheduled value, f_a^{meas} denote the measured area frequency, and f_{norm} denote the nominal system frequency. Let $\mathcal{A}$ denote the set of all BA areas in the interconnected power system. Then, the ACE of each area $a \in \mathcal{A}$ is defined as

$$ACE_a = \sum_{a' \in \mathcal{A}_a} (P_{aa'}^{meas} - P_{aa'}^{sch}) + b_a(f_a^{meas} - f_{norm}), \forall a \in \mathcal{A}, \tag{2}$$

where b_a is the bias factor, and $\mathcal{A}_a$ denotes the set of BA areas that are connected to area a through tie lines.

In this work, we adopt the AGC control logic described in [2]. To this end, we define a state variable, z_a, for each area $a \in \mathcal{A}$, which is the sum of the set point values of participating generators in area a. The evolution of z_a is then described by

$$\dot{z}_a = -z_a - ACE_a + \sum_{i \in \mathcal{G}_a} P_{G_i}^{meas}, \tag{3}$$

where $\mathcal{G}_a$ is the set of generators in area a that participate in AGC, and $P_{G_i}^{meas}$ is the measured power output of generator i in $\mathcal{G}_a$. For each generator $i \in \mathcal{G}_a$, the set point P_i^{ref} is proportional to z_a, i.e., $P_i^{ref} = \kappa_{a_i} z_a$, where the participation factors κ_{a_i}'s satisfy $\sum_{i \in \mathcal{G}_a} \kappa_{a_i} = 1$.

Then, as defined in (1), the set points form u, i.e., $u = \{P_i^{ref}\}_{i \in \mathcal{G}_a, a \in \mathcal{A}} \in \mathbb{R}^l$. Similarly, by stacking the AGC state variables, we form $z = \{z_a\}_{a \in \mathcal{A}} \in \mathbb{R}^p$. Let γ^{meas} denote the set of all measurement variables as $\gamma^{meas} := \{f_a^{meas}, P_{G_i}^{meas}, P_{aa'}^{meas}\}_{a \in \mathcal{A}, a' \in \mathcal{A}_a, i \in \mathcal{G}_a} \in \mathbb{R}^q$. Then, the AGC system can be described compactly as follows:

$$\dot{z} = h_1(\beta^{meas}, z), \tag{4a}$$

$$u = k(z), \tag{4b}$$

with $h_1 : \mathbb{R}^{p+q} \mapsto \mathbb{R}^p$ and $k : \mathbb{R}^p \mapsto \mathbb{R}^l$.

C. Measurement Model

Next, we present the measurement error models considered in this paper. Two types of common deterministic errors have been categorized in [10]. In this paper, we generalize these deterministic errors and consider their corresponding random counterparts.

1) Deterministic errors: Two types of errors are considered. The first type of error is the one that shifts the true value of measurement i by a constant value $\alpha_{1,i}$, i.e.,

$$\beta_{1,i}^{meas} = \beta_i + \alpha_{1,i}, \tag{5}$$

where β_i is the actual value. The second type is called scaling error and is characterized as follows:

$$\beta_{2,i}^{meas} = \beta_i + \alpha_{2,i}\beta_i, \tag{6}$$

where $\alpha_{2,i} \in \mathbb{R}$.

2) Random errors: Like the deterministic error in 5, a random error that shifts the true value of measurement i can be described as

$$\beta_{3,i}^{meas} = \beta_i + \alpha_{3,i}\dot{w}_i, \tag{7}$$

where w_i is a Wiener process and $\alpha_{3,i} \in \mathbb{R}$. Note that this type of error essentially represents white noise because white noise can be viewed as the generalized mean-square derivative of the Wiener process [15]. Similarly, like the type of deterministic error in 6, a random error that results in the scaling of measurement i can be described as follows:

$$\beta_{4,i}^{meas} = \beta_i + \alpha_{4,i}\beta_i\dot{w}_i, \tag{8}$$

where $\alpha_{4,i} \in \mathbb{R}$.

3) General model : The measurement variables that are used as inputs to the AGC system can be expressed as a function of the dynamic state x and the system algebraic state y. Note that although the derivative of bus voltage angles may appear when calculating the area frequency, the derivative of y can be expressed as an algebraic function of x and y by using (1). Assume that there are r measurements corrupted by random errors as described by the models in (7) and (8). Then, the measurement model can be generalized and expressed in a compact form as

$$\beta^{meas} = h_2(x, y) + \sum_{i=1}^{r} \eta_i(x, y)\dot{w}_i, \tag{9}$$

where $h_2 : \mathbb{R}^{n+m} \mapsto \mathbb{R}^q$ captures the actual measurement values and deterministic errors, w_i's are independent Wiener processes, and $\eta_i : \mathbb{R}^{n+m} \mapsto \mathbb{R}^q$ maps to a zero vector except for one nonzero element that represents the intensity of the corresponding random error term.

Note that while in this paper we restrict the analysis to the error models in (5)-(8), it is possible to generalize these further. For instance, as long as the errors can be formulated as continuous deterministic processes or other stochastic processes driven by Wiener processes, the same analysis method still applies. For example, for the errors caused by replay attacks (see, e.g., [16]), the same analysis process follows, except that the system stability will be evaluated in the s-domain by using Laplace transform due to the time delay appeared in the system model. Also for errors that are described by nonlinear functions of the measurement variables, the error can still be described by the general model in (9), and the same analysis procedure applies.

III. Assessing the Impact of Measurement Errors

In this section, we develop a method to assess the impact on power system dynamic performance of the measurement errors discussed in Section II. In this method, the DAE model consisting of (1), (4) and (9) is first linearized along a nominal trajectory to form a linear stochastic differential equation (SDE) model. Then, stochastic system analysis techniques are used to investigate the impact of random measurement errors.

A. Linearization

Assuming the power system with AGC described by (1), (4) and (9) evolves from a set of initial condition and the measurements are error free, a nominal trajectory $(x^*(t), y^*(t), z^*(t), \beta^*(t), u^*(t))$ results. As a consequence of measurement errors, the trajectory is perturbed from its nominal value as follows: $x(t) = x^*(t) + \Delta x(t)$, $y(t) = y^*(t) + \Delta y(t)$, $z(t) = z^*(t) + \Delta z(t)$, $\beta(t) = \beta^*(t) + \Delta\beta(t)$, $u(t) = u^*(t) + \Delta u(t)$. Assume that the functions f, g, h_1, k, h_2 are continuously differentiable with respect to their arguments, and the Jacobian of $g(\cdot)$ in (1b) with respect to y is always invertable along the trajectories. [The implicit function theorem then ensures the existence of an explicit relation between $y(t)$ and $x(t)$.] For notational convenience, we drop the dependence on t in subsequent developments. Then, by linearizing the model along the nominal trajectory, and substituting the algebraic states into the differential equations, we can obtain a linear stochastic differential equation (SDE) model of the form

$$\frac{dX}{dt} = AX + \sum_{i=1}^{r} B_i\eta_i\dot{w}_i, \tag{10}$$

where $X = [\Delta x^T, \Delta z^T]^T \in \mathbb{R}^{n+p}$. Note that the impact of deterministic errors is captured in the matrix A. If A possesses eigenvalues with positive real parts, it suggests that the considered measurement error causes the system to become unstable.

Note that because there are physical and logical constraints on certain variables that are not considered in the linearized model, in practice, the measurement errors will not cause system state variables to diverge without limits. However, these errors will still cause degraded system performance, which will trigger other protection mechanisms. For instance, if the system frequency keeps being outside of the threshold, load shedding or generator tripping may be triggered by under-frequency or over-frequency protection relays.

B. Statistical Moment Analysis

In order to evaluate the impact of random measurement errors, we can apply Dynkin's formula (see, e.g., [12]) to obtain a set of ordinary differential equations (ODEs) describing the dynamics of statistical moments (up to arbitrary order) of the system state variables. In this work, we focus on the evolution of the state mean and covariance; the explicit derivation of the equations that govern these can be found in [17].

1) The impact of random error with constant intensity: For the error model described in (7), since $\alpha_{3,i}$ is a constant, η_i maps to a constant vector. Then, we have that the first and second moments of X in (10) evolve according to

$$\frac{d\mathbb{E}[X]}{dt} = A\mathbb{E}[X], \tag{11a}$$

$$\frac{d\Sigma}{dt} = A\Sigma + \Sigma A^T + B_1\eta_1\eta_1^T B_1^T, \tag{11b}$$

where $\Sigma = \mathbb{E}[XX^T]$.

Assume the original system without measurement errors is stable, meaning that the real parts of the eigenvalues of A are negative. Equation (11a) shows that the state mean is not

affected by the error term and converges to zero eventually. Letting the left-hand side of (11b) be zero results in a Lyapunov equation. Since matrix $B_1\eta_1\eta_1^T B_1^T$ is symmetric and positive definite, the Lyapunov stability theorem guarantees that there exists a positive definite matrix Σ satisfying this Lyapunov equation [18], meaning that the covariance matrix steady-state value exists and is finite.

2) The impact of random error with scaling intensity: Here, we show that the random error model in (8) may cause the system state covariance matrix to become unstable, which means that the system will not converge in the mean square sense and the realized system sample path will be unstable [19]. To this end, let $\Delta\beta_i = \Delta\beta_i + \alpha_{4,i}\Delta\beta_i\dot{w}_i$. Through linearization and substitution of algebraic states using the power flow equations, we can obtain that η_1 can be evaluated as:

$$\eta_1 = \alpha_{4,1}H_1X,$$

where $H_1 \in \mathbb{R}^{q\times(n+p)}$. Then (10) becomes

$$\dot{X} = AX + \alpha_{4,1}B_1H_1X\dot{w}_1 := AX + \alpha_{4,1}\hat{B}_1X\dot{w}_1, \quad (12)$$

where $\hat{B}_1 \in \mathbb{R}^{(n+p)\times(n+p)}$ equals B_1H_1.

The equations governing the evolution of the first and second moments of X are given by

$$\frac{d\mathbb{E}[X]}{dt} = A\mathbb{E}[X], \quad (13a)$$

$$\frac{d\Sigma}{dt} = A\Sigma + \Sigma A^T + \alpha_{4,1}^2\hat{B}_1\Sigma\hat{B}_1{}^T. \quad (13b)$$

In this case, it is possible that the system (13b) is unstable due to $\alpha_{4,1}^2\hat{B}_1\Sigma\hat{B}_1{}^T$. In order to evaluate the effects on system stability, we rearrange the entries of the matrix Σ into a vector Φ. Define the ith row of Σ by Σ_i; then $\Phi = [\Sigma_1\Sigma_2\cdots\Sigma_{n+p}]^T$. Thus, equation (13b) can be rewritten as

$$\frac{d\Phi}{dt} = D\Phi, \quad (14)$$

where $D = I\otimes A + A\otimes I + \alpha_{4,1}^2\hat{B}_1\otimes\hat{B}_1$, I denotes a $(n+p)\times(n+p)$ identity matrix, and $\otimes$ denotes the Kronecker product [20]. By properly choosing $\alpha_{4,1}$, it is possible to make positive the real part of some of the eigenvalues of D, which would cause the system to become unstable. Note that at this point, even though the system state mean is stable; the system state covariance becomes unstable. Eventually, this causes the divergence of system states in a realized sample path.

3) The impact of multiple general random errors: Note that besides these two common types of random errors described earlier, for any continuous error function η_i's, the same method applies. For multiple measurement errors, (13b) becomes

$$\frac{d\Sigma}{dt} = A\Sigma + \Sigma A^T + \sum_{i=1}^{r}\alpha_{4,i}^2\hat{B}_i\Sigma\hat{B}_i^T,$$

where $\hat{B}_i = 0$ if η_i maps to a constant vector. The effects on system stability can be evaluated by following the aforementioned procedure of constructing (14); the matrix D in (14) is determined based on the scaling parameters, i.e., $\alpha_{4,i}$'s.

IV. Analysis with Reduced-Order Models

In this section, we utilize singular perturbation arguments (see, e.g., [21], [22]) to derive a reduced-order model of the system dynamics. With this simplified model, we are able to (i) explicitly investigate the impact of different erroneous measurements (e.g., erroneous frequency measurement, and erroneous generation output measurements); and (ii) estimate the range of parameter values that will make the system fail to perform satisfactorily.

A. Reduced-Order Dynamic Model

We assume that the time constants associated with the electromechanical dynamics are much smaller than those associated with the AGC system. Therefore, the time scales of these two subsystems can be decoupled, and we expect the AGC dynamics to dominate the system dynamic behavior in the time scale of interest. [Similar argument has been utilized in AGC system studies; see, e.g., [23].] Then, the set of DAEs that describes the electromechanical dynamics are converted to algebraic equations by setting the left-hand side of (1) to be zero, and a reduced-order model is obtained. Note that one may argue that this assumption is not totally valid due to the high inertia of some generators in the bulk power system. However, although there is small discrepancy between the trajectory that results from the full-order model and the trajectory that results from the reduced-order model, the stability properties are preserved between the full- and reduced-order models given the original system (1) is stable, meaning that if the measurement error destabilizes the reduced-order model, it will destabilize the original system as well, and vice versa. This claim follows from the result of Theorem 5.1 in [22], which states that the difference between the full-order model trajectory and that of the reduced-order model is on the order of the magnitude of the ratio of the fast and slow subsystem time constants; therefore the difference is bounded. In addition, we assume that the transmission network is lossless, which implies that the total generation output is equal to the total demand, i.e., $\sum_{i\in\mathcal{G}}P_{G_i} = \sum_{j\in\mathcal{D}}P_{D_j}$, where $\mathcal{G}$ indicates the set of all generators, P_{G_i} denotes the electrical output of generator i, $\mathcal{D}$ indicates the set of all the loads in the power system, and P_{D_j} denotes the demand at load j. With these three assumptions, a reduced-order dynamic model can be derived.

Let P_i denote the turbine power, and P_i^{ref} denote the generator set point of unit i. Then, the inertia response and governor response of unit i is given by (see, e.g., [24]):

$$M_i\frac{d\omega_i}{dt} = P_i - P_{G_i} - D_i(\omega_i - \omega_s), \quad (15a)$$

$$T_i\frac{dP_i}{dt} = -P_i + P_i^{ref} - \frac{1}{R_i}(\omega_i - \omega_s), \quad (15b)$$

where ω_i is the machine electrical rotational speed, while w_s is the system synchronous speed; D_i is the damping coefficient; M_i is the scaled machine inertia constant; T_i is the governor time constant; the gain R_i determines the slope of the governor droop characteristic; and P_{G_i} is the power output.

In steady state, the left-hand side of (15) is set to zero, and the governor control induces a steady-state error in the

frequency, which causes all generators to rotate at the same speed, i.e., $\omega_i = \omega_o, \forall i \in \mathcal{G}$. Then, by summing (15) over all generators, the following algebraic relationship can be obtained:

$$z - \sum_{i\in\mathcal{G}} P_{G_i} = \beta \Delta f, \tag{16}$$

where $\Delta f = (\omega_o - \omega_s)/2/\pi$, and $\beta = 2\pi \sum_{i\in\mathcal{G}} (\frac{1}{R_i} + D_i)$, which is called the frequency response characteristic [25]. Then, by solving for Δf, we obtain

$$\Delta f = \frac{z - \sum_{i\in\mathcal{G}} P_{G_i}}{\beta}. \tag{17}$$

Without loss of generality, we focus on the case of a single BA area and drop the subscript that indicates the BA area in the following developments. Then, we have that $ACE = b\Delta f$, and

$$\dot{z} = -z - b\Delta f + \sum_{i\in\mathcal{G}} P_{G_i}. \tag{18}$$

Plugging (17) into (18) and utilizing the lossless transmission network assumption, we obtain that

$$\dot{z} = -\frac{b+\beta}{\beta}(z - \sum_{i\in\mathcal{D}} P_{D_i}).$$

If b is set to be β as suggested in [25], the AGC dynamic model becomes $\dot{z} = -2z + 2\sum_{i\in\mathcal{D}} P_{D_i}$, which is a stable ODE.

B. Impact of Erroneous Frequency Measurement

As discussed earlier, since the errors described in (5) and (7) will not affect system stability in the mean square sense, we mainly focus on the impact of the scaling errors in (6) and (8). Assume that there is a scaling error in the frequency measurement, $f^{meas} = f + \alpha_2 \Delta f$ (i.e., $\Delta f^{meas} = \Delta f + \alpha_2 \Delta f$). Then, by replacing the true frequency value with the erroneous measurement in (18), we obtain that

$$\dot{z} = -\frac{b(1+\alpha_2)+\beta}{\beta}(z - \sum_{i\in\mathcal{D}} P_{D_i}). \tag{19}$$

Now, if $\alpha_2 < -\frac{\beta}{b} - 1$, the system in (19) becomes unstable. Note that if $b = \beta$, then a value of α_2 smaller than -2 means that the measured frequency deviation, Δf, has the opposite sign to that of the correct value.

Assume the error is of random nature and can be described by the model in (8), i.e., $f^{meas} = f + \alpha_4 \Delta f \dot{w}$. Then, by replacing the error-free frequency measurement in (18) with this erroneous measurement model, we obtain

$$\begin{aligned}\dot{z} &= -(b+\beta)\Delta f - b\alpha_4 \Delta f \dot{w} \\ &= -\frac{b+\beta}{\beta}(z - \sum_{i\in\mathcal{D}} P_{D_i}) - \frac{b\alpha_4}{\beta}(z - \sum_{i\in\mathcal{D}} P_{D_i})\dot{w}.\end{aligned} \tag{20}$$

Referring to the analysis in Section III, we can see that if $|\alpha_4| > \sqrt{\frac{2(b+\beta)\beta}{b^2}}$, the system in (20) does not converge in the mean square sense.

C. Impact of Erroneous Generation Output Measurement

Assume that there are deterministic errors in the output measurement of generator k, i.e., $P_{G_k}^{meas} = P_{G_k} + \alpha_2 P_{G_k}$, and the participation factor of this generator is κ_k. Then, from (17), we obtain that

$$P_{G_k} = \kappa_k z - (\frac{1}{R_k} + D_k) 2\pi \Delta f.$$

Then, the total generation output measurement is

$$\begin{aligned}\sum_{i\in\mathcal{G}} P_{G_i}^{meas} &= P_{G_k}^{meas} + \sum_{i\neq k} P_{G_i} \\ &= z - \beta\Delta f + \alpha_2(\kappa_k z - (\frac{1}{R_k} + D_k)2\pi\Delta f).\end{aligned}$$

Replacing the actual generation output value with that resulting from an erroneous measurement, we have

$$\dot{z} = (\alpha_2\kappa_k - \xi)z - \xi \sum_{i\in\mathcal{D}} P_{D_i}, \tag{21}$$

where $\xi = \frac{b+\beta+2\pi\alpha_2(\frac{1}{R_k}+D_k)}{\beta}$.

For $\alpha_2 > \frac{b+\beta}{\beta\kappa_k - (\frac{1}{R_k}+D_k)}$, the AGC system becomes unstable. Note that if $\kappa_k = \frac{\frac{1}{R_k}+D_k}{\sum_i \frac{1}{R_i}+D_i}$, there exists no α_2 that destabilizes the system. However, this error can make the system frequency converge to an unacceptable value (e.g., below a certain threshold that triggers load shedding schemes). By setting the right-hand side of (21) to zero, the frequency deviation in steady state is $\frac{\alpha_2\kappa_k \sum P_{G_i}}{b+\beta-\alpha_2(\kappa_k\beta - \frac{1}{R_k} - D_k)}$. Note that this frequency deviation value is proportional to the total value of the demand, which can be very large. As shown in the case study section, this error can easily make the system frequency go beyond the acceptable threshold.

If the error is of random nature and is described in (8), i.e., $P_{G_k}^{meas} = P_{G_k} + \alpha_4 P_{G_k} \dot{w}$, we have

$$\dot{z} = -\frac{b+\beta}{\beta}(z - \sum_{i\in\mathcal{D}} P_{D_i}) + \zeta(z)\dot{w}, \tag{22}$$

where $\zeta(z) = \alpha_4(\kappa_k - \frac{\frac{1}{R_k}+D_k}{\beta})z + \alpha_4 \frac{\frac{1}{R_k}+D_k}{\beta} \sum_{i\in\mathcal{D}} P_{D_i}$. Denote $C_1 = -\frac{b+\beta}{\beta}, C_2 = \alpha_4\kappa_k - \alpha_4\frac{\frac{1}{R_k}+D_k}{\beta}$, and $C_3 = \frac{\alpha_4\kappa_k \sum_{i\in\mathcal{D}} P_{D_i}}{\beta}$. Using the method described in Section III, we obtain that

$$\begin{aligned}\frac{d\mathbb{E}[\Delta f]}{dt} &= C_1\mathbb{E}[\Delta f], \\ \frac{d\mathbb{E}[\Delta f^2]}{dt} &= (2C_1 + C_2^2)\mathbb{E}[\Delta f^2] + +2C_2C_3\mathbb{E}[\Delta f] + C_3^2,\end{aligned}$$

from which, we can see that the frequency mean converges to zero. If $2C_1 + C_2^2 > 0$, the system becomes unstable in the mean square sense; otherwise, the frequency variance converges to a nonzero value, $-\frac{C_3^2}{2C_1+C_2^2}$, which may cause violations of some frequency requirement standards, e.g., CPS1 [26].

D. Two-Area System Reduced-Order Model

A similar procedure is also applicable to a two-area system. In this case, the dynamics of the AGC variables are given by:

$$\dot{z}_1 = -z_1 - ACE_1 + \sum_{i\in\mathcal{G}_1} P_{G_i}^{meas}, \tag{23a}$$

$$\dot{z}_2 = -z_2 - ACE_2 + \sum_{j\in\mathcal{G}_2} P_{G_j}^{meas}, \tag{23b}$$

where

$$ACE_1 = P_{12}^{meas} - P_{12}^{sch} + b_1(f_1^{meas} - f_{norm}),$$
$$ACE_2 = P_{21}^{meas} - P_{21}^{sch} + b_2(f_2^{meas} - f_{norm}).$$

By assuming that $f_1 = f_2$, and similar to (16), we have that:

$$z_1 - \sum_{i\in\mathcal{G}_1} P_{G_i} = \beta_1 \Delta f, \tag{24a}$$

$$z_2 - \sum_{j\in\mathcal{G}_2} P_{G_j} = \beta_2 \Delta f, \tag{24b}$$

where $\beta_1 = \sum_{i\in\mathcal{G}_1}(\frac{1}{R_i} + D_i)$, and $\beta_2 = \sum_{j\in\mathcal{G}_2}(\frac{1}{R_j} + D_j)$.

Again, assuming that the transmission network is lossless, we have that

$$\sum_{i\in\mathcal{G}_1} P_{G_i} = \sum_{i\in\mathcal{D}_1} P_{D_i} + P_{12}, \tag{25a}$$

$$\sum_{j\in\mathcal{G}_2} P_{G_j} = \sum_{j\in\mathcal{D}_2} P_{D_j} + P_{21}, \tag{25b}$$

$$P_{12} = -P_{21}. \tag{25c}$$

Plugging (25) into (24), we can solve for Δf and P_{12}:

$$\Delta f = \frac{1}{\beta_1+\beta_2}(z_1 + z_2 - \sum_{i\in\mathcal{D}} P_{D_i}); \tag{26a}$$

$$P_{12} = \frac{\beta_1}{\beta_1+\beta_2}(z_1 - \sum_{i\in\mathcal{D}_1} P_{D_i}) - \frac{\beta_2}{\beta_1+\beta_2}(z_2 - \sum_{j\in\mathcal{D}_2} P_{D_j}). \tag{26b}$$

Then, if there are no measurement errors, by substituting (26) into (23), the dynamics of the AGC variables becomes

$$\dot{z}_1 = -\frac{\beta_1+\beta_2+b_1}{\beta_1+\beta_2} z_1 - \frac{b_1}{\beta_1+\beta_2} z_2 + \frac{\beta_1+\beta_2+b_1}{\beta_1+\beta_2} \sum_{i\in\mathcal{D}_1} P_{D_i} + \frac{b_1}{\beta_1+\beta_2} \sum_{j\in\mathcal{D}_2} P_{D_j} + P_{12}^{sch},$$

$$\dot{z}_2 = -\frac{\beta_1+\beta_2+b_2}{\beta_1+\beta_2} z_2 - \frac{b_2}{\beta_1+\beta_2} z_1 + \frac{\beta_1+\beta_2+b_2}{\beta_1+\beta_2} \sum_{j\in\mathcal{D}_2} P_{D_j} + \frac{b_2}{\beta_1+\beta_2} \sum_{i\in\mathcal{D}_1} P_{D_i} + P_{21}^{sch}.$$

Here we can see that the system is stable as the two eigenvalues are -1 and $-1 - \frac{b_1+b_2}{\beta_1+\beta_2}$.

Following the same procedure as in Sections IV.B and IV.C, we can evaluate the impact of errors in various measurements. For instance, we can show that if there are scaling errors in the frequency measurements of both areas, $f_1^{meas} = f + \alpha_{2,1}\Delta f$, $f_2^{meas} = f + \alpha_{2,2}\Delta f$, the dynamics of AGC variables becomes

$$\dot{z}_1 = -\frac{\beta_1+\beta_2+b_1(1+\alpha_{2,1})}{\beta_1+\beta_2} z_1 - \frac{b_1(1+\alpha_{2,1})}{\beta_1+\beta_2} z_2 + \frac{\beta_1+\beta_2+b_1(1+\alpha_{2,1})}{\beta_1+\beta_2} \sum_{i\in\mathcal{D}_1} P_{D_i} + \frac{b_1(1+\alpha_{2,1})}{\beta_1+\beta_2} \sum_{j\in\mathcal{D}_2} P_{D_j} + P_{12}^{sch}, \tag{27a}$$

$$\dot{z}_2 = -\frac{\beta_1+\beta_2+b_2(1+\alpha_{2,2})}{\beta_1+\beta_2} z_2 - \frac{b_2(1+\alpha_{2,2})}{\beta_1+\beta_2} z_1 + \frac{\beta_1+\beta_2+b_2(1+\alpha_{2,2})}{\beta_1+\beta_2} \sum_{j\in\mathcal{D}_2} P_{D_j} + \frac{b_2(1+\alpha_{2,2})}{\beta_1+\beta_2} \sum_{i\in\mathcal{D}_1} P_{D_i} + P_{21}^{sch}. \tag{27b}$$

Then, if $\alpha_{2,1} < -1 - \frac{\beta_1}{b_1}$ and $\alpha_{2,2} < -1 - \frac{\beta_2}{b_2}$, one of the two eigenvalues becomes positive; thus, the system in (27) becomes unstable. If there is a scaling error in the frequency measurement of one area, $f_1^{meas} = f + \alpha_{2,1}\Delta f$, similarly, we can show that if $\alpha_{2,1} < -1 - \frac{\beta_1+\beta_2+b_2}{b_1}$, one of the two eigenvalues becomes positive; thus, the system becomes unstable.

Similarly, if there are scaling errors in the interchange power measurements, $P_{12}^{meas} = P_{12} + \alpha_{2,3}P_{12}$, replacing the true measurement with the erroneous measurement in (23), the dynamics of z_1 becomes

$$\dot{z}_1 = -\frac{\beta_1+\beta_2(1+\alpha_{2,3})+b_1}{\beta_1+\beta_2} z_1 - \frac{b_1-\alpha_{2,3}\beta_1}{\beta_1+\beta_2} z_2 \tag{28a}$$

$$+ \frac{\beta_1+\beta_2(1+\alpha_{2,3})+b_1}{\beta_1+\beta_2} \sum_{i\in\mathcal{D}_1} P_{D_i} \tag{28b}$$

$$+ \frac{b_1-\alpha_{2,3}\beta_1}{\beta_1+\beta_2} \sum_{j\in\mathcal{D}_2} P_{D_j} + P_{12}^{sch}. \tag{28c}$$

Again by checking the values of the eigenvalues, we can determine whether or not the measurement error destabilizes the system. If not, we can also check whether the measurement error makes the system frequency converge to an unacceptable value by setting the left-hand side of (28) to zero and solving for the steady-state values of z_1, z_2 and Δf.

V. Discussions with Practical AGC Systems

In this section, we discuss the impact of measurement errors in the context of practical AGC systems, where AGC suspension mechanisms are implemented. From a defense point of view, we also discuss the challenge of detecting measurement errors in SCADA systems and propose ideas to address this challenge by integrating the SCADA system with the wide area measurement system (WAMS).

A. AGC with Suspension Schemes and Load Shedding

In practice, some AGC implementation guidelines are recommended in order to limit the impact of erroneous measurements and emergency events. The western electricity coordinating council (WECC) suggests that AGC suspension should

be considered when the system frequency deviation is greater than a threshold, f_{agc} [27]. At the same time, underfrequency load shedding relays are commonly installed to shed load when the frequency is below a threshold, f_{ld} [10]. In this regard, if the frequency measurement used by AGC reaches the threshold f_{agc} before the actual frequency falls below f_{ld}, AGC will be suspended, and the impact on system performance will be limited. On the other hand, if the actual frequency falls below the threshold f_{ld} before AGC is suspended, the low frequency value will trigger load shedding. Therefore, for the deterministic scaling attack on the frequency measurements to cause a severe impact, it must be engineered in such a way that the erroneous measurement does not trigger the AGC suspension, i.e.,

$$|\Delta f^{meas}| = |\Delta f + \alpha_2 \Delta f| < f_{agc},$$

when the actual frequency reaches the limit to trigger load shedding, i.e.,

$$f_{norm} + \Delta f = f_{ld},$$

which gives an extra constraint on the parameter α_2: $\alpha_2 < -1 + \frac{f_{agc}}{f_{ld} - f_{norm}}$.

For the case of a random attack, there is a non-zero probability that the erroneous frequency measurements will reach the suspension threshold f_{agc}. However, WECC also recommends that the lower-than-threshold condition should be verified for a few of the AGC execution cycles before actually suspending it, in order to avoid frequent suspension. Taking this into account, the probability for erroneous frequency measurements to be consecutively lower than the threshold is very small. Therefore, it is still very likely that such attacks would cause serious impacts on system operations.

B. Error Detection and Mitigation

Even with the current AGC suspension protection mechanism described above, the aforementioned potential severe impact of erroneous measurements highlights the importance of integrity in the measurements used by AGC systems. Thus, error detection methods are required to maintain measurement integrity.

The integrity of power measurements can be protected by bad data detection mechanisms implemented in the SCADA system state estimation process; this has been extensively studied (see, e.g., [28]). However, it is difficult to ensure the integrity of frequency measurements because the frequency variable is not included in the SCADA steady-state estimation process. One way to address this issue, implied by the steady-state study on AGC attacks in [23], is to utilize the steady-state relationship between the power mismatch and the frequency in (17). However, since this is based on the reduced-order model obtained via singular perturbation, this method may not be accurate when system dynamics are considered.

Another method is to incorporate synchrophasor measurements, provided by phasor measurement units (PMUs) in the wide-area measurement system (WAMS), into the SCADA system. One intuitive way is to compare frequency measurements from the SCADA system with those measured by PMUs. But when there is a discrepancy, it is difficult to determine which ones should be trusted. To address this issue, we utilize the fact that PMUs measure frequencies based on the derivative of phase angles, the integrity of which can be detected via state estimation in the SCADA system. In other words, PMU relates the frequency measurements with the variables that are used in the SCADA state estimator. If the frequency measurement from a PMU is offset, the phasor angle measurement will also be inaccurate. This can be directly detected through the bad data detection algorithms in the state estimator. Consider an error ϵ is introduced to the PMU frequency measurement. It will cause an error of $360T\epsilon$ degrees in the angle measurement for a short period of time T, which will be well beyond the tolerance margin of the bad data detection algorithm. Therefore, the errors added to the frequency measurements can be detected by integrating SCADA and WAMS systems.

VI. Case Studies

In this section, we demonstrate the impact of the aforementioned measurement errors on a 68-bus 16-machine system, which is a representative model of the New England/New York interconnected power system. Its one-line diagram and detailed description can be found in [29]. Each of the 16 generator units is modeled by a combination of a synchronous machine model, an exciter model, a power system stabilizer model, and a turbine/governor model. We utilized the MATLAB-based Power System Toolbox (PST) to implement the AGC algorithms and simulate the system dynamics. The data of this system is part of the PST suite and can be found in [30]. The linearized system is also obtained by making use of the the small-signal analysis function provided in PST. The eigenvalue corresponding to the AGC system is -0.001, while the largest one of the rest eigenvalues that correspond to the system electromechanical dynamics is -0.1004. The high ratio of these two eigenvalues supports the singular perturbation argument utilized in Section IV to derive a reduced-order model. In addition, we also validate the resulting reduced-order model by comparing the critical error parameter values obtained using the full- and reduced-order models respectively.

A. Accuracy of the Linearized Model

Before proceeding with the impact analysis, we first verify the accuracy of our linearization procedure when utilized to study the New England/New York system model with AGC. To this end, we consider two scenarios and compare the trajectories obtained by simulating the nonlinear system model with those obtained through the linearized model.

First, we assume that there is a 0.1 p.u. variation from the nominal value in each load. We plot the resulting trajectories of the frequency deviation obtained with the nonlinear and linearized models in Fig. 1(a). In the second scenario, we assume that there are random errors in the frequency measurements. The measurement error is assumed to be white noise. The results are shown in Fig. 1(b), where we plot one sample path of the resulting frequency deviation trajectories obtained with the nonlinear model and linearized models. As one can see, in both cases the linearized system trajectory approximates the nonlinear system trajectory closely.

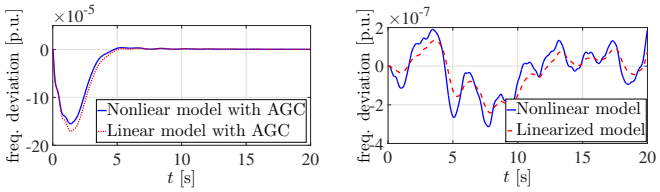

(a) Frequency deviation with load variation.

(b) Frequency deviation with white noise errors.

Figure 1: Validation of linearization process.

B. Impact of Deterministic Errors

1) Impact of erroneous frequency measurement: We focus on the impact of the scaling errors discussed in Section IV-B. First from the reduced-order model in (18), we obtain that the error parameter α_2 should be less than -2 in order for the system to become unstable. With the full-order model described in (1), (4) and (9), after linearization and checking the eigenvalues of the matrix in (10), we find that with the error parameter being less than -1.98, the system becomes unstable. The small mismatch may come from the lossless network assumption. The relationship between the maximum real part of the eigenvalues and the error parameter is depicted in Fig. 2(a). Note that due to the fact that there is always a theoretical zero eigenvalue (a result of choosing one angle variable as the reference angle in PST), the maximum eigenvalue is zero when the system is stable. We also vary the system operating point by randomly changing the load and generation values 100 times. At each time, the load and generation values at each bus are multiplied by a independent random variable, which is uniformly distributed between 0.5 and 1.2. Except for the cases that are not feasible (i.e., no power flow solutions), the critical point stays at -1.98 for all the other cases as shown in Fig. 2(b). Choose $\alpha_2 = 2.1$, and the full-order model is used in the simulation. The resulting system frequency and the AGC variable z (i.e., the sum of the generators' set points) are depicted by the red dashed line in Fig. 3, which illustrates that the system becomes unstable.

Note that in practice, the AGC is implemented in discrete time; thus we also simulate the system performance with a discrete implementation of the AGC model with a sample-and-hold period of 2s, and the results are plotted by the blue solid line in Fig. 3 as well, which shows that the system is unstable and the system variables even diverge more severely. In the remainder, we simulate the AGC dynamics according to a discrete-time implementation of a continuous-time model, which makes the system response faster than that of the conventional sample-and-hold based AGC implementation. However, the stability characteristics hold the same for systems with AGC operated in continuous time and discrete time.

2) Impact of erroneous generation output measurement: Deterministic errors are added to the generation output measurement. The results of our experiments are consistent with the analysis on the generation measurement errors in Section IV-C. This type of error does not destabilize the system when described by the linear model or the full-order model.

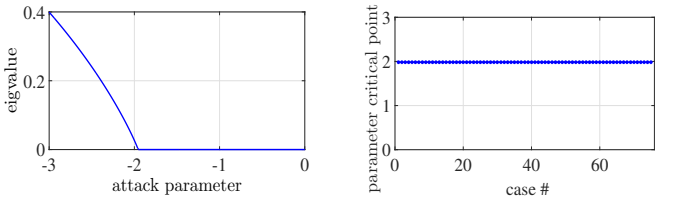

(a) Eigenvalues for base case.

(b) Critical points for various cases.

Figure 2: Eigenvalue.

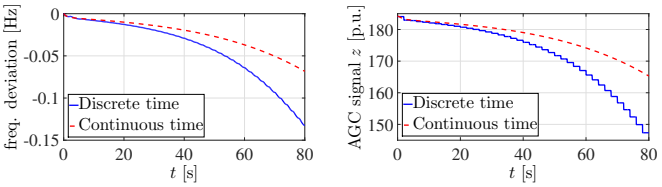

(a) System frequency.

(b) AGC variable z.

Figure 3: Deterministic error in frequency measurement.

But the error will drive the system frequency beyond the satisfactory region (here we consider frequency deviation being smaller than 0.05 Hz as satisfactory performance). For this system, if the scaling error with α_2 being 0.061 is introduced in the generation output measurement of generation unit 16, the dynamics of the system variables (i.e., the system frequency and the AGC variable z) are depicted in Fig. 4, where one can see that the system converges to a steady state. However, the absolute value of the system frequency deviation stays larger than 0.05 Hz. Also note that the critical value of α_2 depends on the total value of demand. Therefore, if the power demand in this system is doubled, $\alpha_2 = 0.03$ will drive the system frequency beyond the safety region.

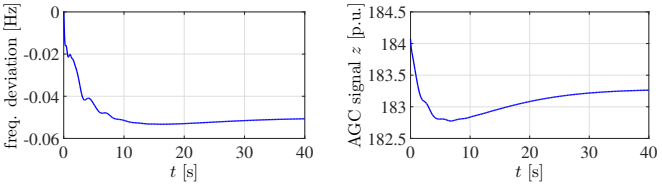

(a) System frequency.

(b) AGC variable z.

Figure 4: Deterministic error in generation measurement.

C. Impact of Random Errors

1) Impact of erroneous frequency measurement: Consider the scaling random error model in (8). First, by using (20), we obtain that the error parameter α_4 should be larger than 2 in order to drive the system to be unstable in the mean square sense. Then, with the full-order model as described in (1), (4) and (9), after linearization and checking the eigenvalues of the matrix in (10), we find that for the error parameter being larger than 2.3, the system becomes unstable in the mean square sense. In order to get the statistics of the system state variables, one can numerically solve the ODEs in (13b) that govern the evolution of state variables' first and second moments. An alternative is to run a Monte Carlo simulation $10,000$ times and estimate the statistics using the resulting $10,000$ sample paths. For $\alpha_4 = 2.4$, the mean and variance of the frequency deviation when using both methods are plotted in Figs. 5(a) and 5(b). The closeness of the results obtained from both methods verifies the accuracy of our stochastic system analysis procedure. The figure also shows that although the mean stays stable, the variance diverges. Thus, the system becomes unstable in the mean square sense. One unstable sample path of the system frequency is depicted in Fig. 5(c).

2) Impact of erroneous generation output measurement: The results of our experiment are consistent with the analysis with the reduced-order model in (22). This type of measurement error does not destabilize the system with either the linear system or the full-order system model in the mean square sense. Following the same Monte Carlo and ODE simulation procedure described above, the mean and variance of the frequency deviation are obtained. The mean converges to zero. Fig. 6(a) depicts the variance when the scaling random error with $\alpha_4 = 0.061$ is injected into the generation output measurement of unit 16. This figure confirms that unlike the impact of random errors in frequency measurements that may destabilize the system, in this case the variance will converge but not zero. One sample path of the frequency deviation is plotted in Fig. 6(b), from which we can observe that although the system converges in the mean square sense, the frequency deviation is still very likely to go beyond the safety region (e.g., smaller than -0.05 Hz) due to the large variance.

VII. Concluding Remarks

This paper proposed a method to assess the impact on power system dynamic performance of various errors in the measurements utilized by the AGC system. With this method, not only can we evaluate the impact of deterministic errors but also that of random errors. We can also identify the critical measurement errors that significantly degrade the system performance and cause the system to become unstable.

We have observed that although AGC is robust to constant intensity (white noise) errors, a class of random error with scaling intensity will cause the system to become unstable in the mean square sense (i.e., divergence of the system state for realized sample paths). Also with the reduced-order system model derived, we have observed that scaling (deterministic and random) errors in the frequency measurements can cause the system to become unstable, while errors in the generation output measurements can drive the system to converge to a state that is not satisfactory in terms of performance. The method was applied to a 68-bus New England/New York power system to numerically verify the above statements.

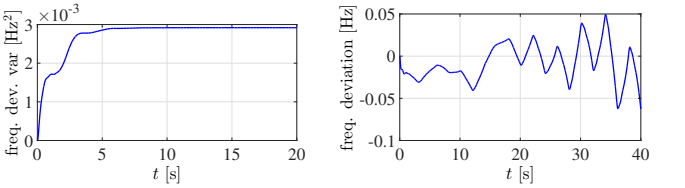

(a) Variance of frequency deviation. (b) Sample path of frequency deviation.

Figure 6: Case with random error in generation measurement.

References

[1] "Vulnerability analysis of energy delivery control systems," Idaho National Laboratory, Sep. 2011. [Online]. Available: http://energy.gov/

[2] A. Wood and B. Wollenberg, *Power Generation, Operation, and Control*. New York, NY: Wiley, 1996.

[3] S. Wang, X. Meng, and T. Chen, "Wide-area control of power systems through delayed network communication," *IEEE Transactions on Control Systems Technology*, vol. 20, no. 2, pp. 495–503, Mar. 2012.

[4] J. Zhang and A. D. Domínguez-García, "On the impact of communication delays on power system automatic generation control performance," in *Proc. of North American Power Symposium*, Sep. 2014.

[5] F. Pasqualetti, F. Dorfler, and F. Bullo, "Attack detection and identification in cyber-physical systems," *IEEE Transactions on Automatic Control*, vol. 58, no. 11, pp. 2715–2729, Nov. 2013.

[6] S. Amin, A. A. Cárdenas, and S. S. Sastry, "Safe and secure networked control systems under denial-of-service attacks," in *Proc. of International Conference on Hybrid Systems: Computation and Control*, 2009.

[7] L. Schenato, B. Sinopoli, M. Franceschetti, K. Poolla, and S. Sastry, "Foundations of control and estimation over lossy networks," *Proceedings of the IEEE*, vol. 95, no. 1, pp. 163–187, Jan. 2007.

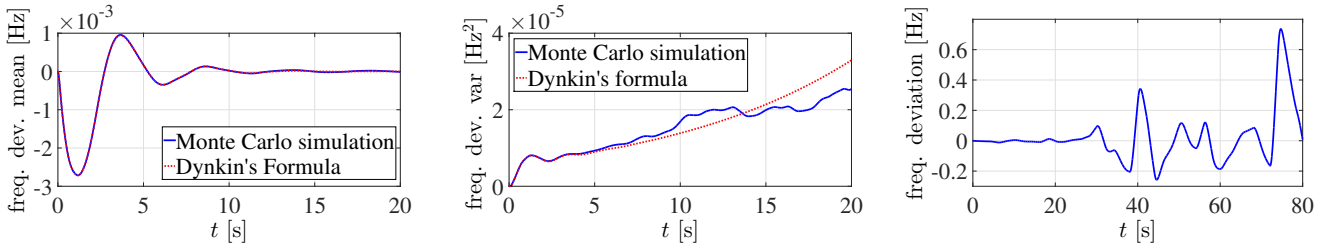

(a) Frequency deviation mean. (b) Frequency deviation variance. (c) Sample path of frequency deviation.

Figure 5: Case with random error in frequency measurement.

[8] Y. Liu, P. Ning, and M. K. Reiter, "False data injection attacks against state estimation in electric power grids," in *Proc. of ACM Conference on Computer and Communications Security*, 2009, pp. 21–32.
[9] L. Xie, Y. Mo, and B. Sinopoli, "False data injection attacks in electricity markets," in *Proc. of IEEE International Conference on Smart Grid Communications*, Oct. 2010, pp. 226–231.
[10] S. Sridhar and G. Manimaran, "Data integrity attacks and their impacts on scada control system," in *Proc. of IEEE Power and Energy Society General Meeting*, Jul. 2010.
[11] J. Zhang and A. D. Domínguez-García, "On the failure of power system automatic generation control due to measurement noise," in *Proc. of IEEE Power and Energy Society General Meeting*, Jul. 2014.
[12] J. Hespanha, "Modeling and analysis of stochastic hybrid systems," *IEE Proceedings - Control Theory and Applications*, vol. 153, no. 5, pp. 520 – 535, Sep. 2006.
[13] P. Sauer and M. Pai, *Power System Dynamics and Stability*. Prentice-Hall, 1998.
[14] Y. Chen and A. Domínguez-García, "A method to study the effect of renewable resource variability on power system dynamics," *IEEE Transactions on Power Systems*, vol. 27, no. 4, pp. 1978–1989, 2012.
[15] B. Øksendal, *Stochastic Differential Equations: An Introduction with Applications*. Springer, 2010.
[16] Y. Mo and B. Sinopoli, "Secure control against replay attacks," in *Proc. of the Allerton Conference on Communication, Control, and Computing*, Sep. 2009, pp. 911–918.
[17] F. Schweppe, *Uncertain dynamic systems*. Prentice-Hall, 1973.
[18] H. Khalil, *Nonlinear Systems*. Prentice-Hall, 2002.
[19] B. Hajek, *An Exploration of Random Processes for Engineers*. [Online] http://www.ifp.illinois.edu/ hajek/Papers/randomprocJan14.pdf, 2014.
[20] R. Horn and C. Johnson, *Topics in Matrix Analysis*. New York, NY: Cambridge University Press, 1991.
[21] R. E. O'Malley and L. R. Anderson, "Time-scale decoupling and order reduction for linear time-varying systems," *Optimal Control Applications and Methods*, vol. 3, no. 2, pp. 133–153, 1982.
[22] P. Kokotovic, H. Khalil, and J. O'Reilly, *Singular Perturbation Methods in Control: Analysis and Design*. Academic Press, 1986.
[23] S. Sridhar and M. Govindarasu, "Model-based attack detection and mitigation for automatic generation control," *IEEE Transactions on Smart Grid*, vol. 5, no. 2, pp. 580–591, Mar. 2014.
[24] A. D. Domínguez-García, "Models for impact assessment of wind-based power generation on frequency control," in *Control and Optimization Methods for Electric Smart Grids, Power Electronics and Power Systems*. Springer-Verlag, 2012.
[25] J. Glover, M. Sama, and T. Overbye, *Power Systems Analysis and Design*. Upper Saddle Rever, NJ: Thompson-Engineering, 2008.
[26] L. Wang and D. Chen, "Extended term dynamic simulation for agc with smart grids," in *Proc. of IEEE Power and Energy Society General Meeting*, Jul. 2011.
[27] "Western electricity coordinating council guidelines for suspending automatic generation control," WECC Operations Committee. [Online]. Available: https://www.wecc.biz/Reliability/Guidelines\%20For\%20Monitoring\%20and\%20scheduling\%20remote\%20generation.pdf
[28] E. Handschin, F. Schweppe, J. Kohlas, and A. Fiechter, "Bad data analysis for power system state estimation," *IEEE Transactions on Power Apparatus and Systems*, vol. 94, no. 2, pp. 329–337, 1975.
[29] G. Rogers, *Power system oscillations*. Kluwer Academic Publishers, 2000.
[30] Power system toolbox. [Online]. Available: http://www.eps.ee.kth.se/personal/vanfretti/pst

Jiangmeng Zhang (S'10) received the B.S. degree in automatic control from Xi'an Jiaotong University, Xi'an, Shaanxi, China, in 2010, and the M.S. and Ph.D. degrees in electrical engineering from the University of Illinois at Urbana-Champaign, Urbana, IL, USA in 2012 and 2016, respectively.

Her research interests include power system analysis, uncertainty impact evaluation, and cyber-physical security. She is currently a quantitative researcher at Citadel with a focus on the uncertainty impact on power and energy markets.

Alejandro D. Domínguez-García (S'02, M'07) received the degree of "Ingeniero Industrial" from the University of Oviedo (Spain) in 2001 and the Ph.D. degree in electrical engineering and computer science from the Massachusetts Institute of Technology, Cambridge, MA, in 2007.

He is an Associate Professor in the Electrical and Computer Engineering Department at the University of Illinois at Urbana-Champaign, where he is affiliated with the Power and Energy Systems area; he also has been a Grainger Associate since August 2011. He is also an Associate Research Professor in the Coordinated Science Laboratory and in the Information Trust Institute, both at the University of Illinois at Urbana-Champaign.

His research interests are in the areas of system reliability theory and control, and their applications to electric power systems, power electronics, and embedded electronic systems for safety-critical/fault-tolerant aircraft, aerospace, and automotive applications.

Dr. Domínguez-García received the National Science Foundation CAREER Award in 2010, and the Young Engineer Award from the IEEE Power and Energy Society in 2012. In 2014, he was invited by the National Academy of Engineering to attend the U.S. Frontiers of Engineering Symposium, and selected by the University of Illinois at Urbana-Champaign Provost to receive a Distinguished Promotion Award. In 2015, he received the U of I College of Engineering DeanÕs Award for Excellence in Research.

He is an editor of the IEEE TRANSACTIONS ON POWER SYSTEMS and the IEEE POWER ENGINEERING LETTERS.